The electron heat transport for high power electron cyclotron heating at the Wendelstein7-AS Stellarator

H.P. Laqua, V.Erckmann, H.Maaßberg, W7-AS Team
Max-Planck-Institut für Plasmaphysik, EURATOM Ass.
D-85748 Garching, FRG,
ECRH-Group
Institut für Plasmaforschung, Univ. Stuttgart, D-70569 Stuttgart, FRG

Abstract

Slow and fast modulation experiments have been performed with an upgraded ECRH power of 2.5 MW. Different transport regimes were found at different radii. With a high resolution ECE-system the sharp transition into the "electron root"-region could be resolved. Inside that region a saturation of the electric field was found.

Introduction

For high power electron cyclotron heating (ECRH) of low density plasmas (long mean free path regime). The electron heat transport is dominating. The electrons are more or less energetically decoupled from the ions, which only guarantee ambipolarity. At different radii the transport is dominated by different mechanism. As shown in Fig. 1 at the low temperature plasma edge, where neo-classical transport becomes small, the turbulent transport is dominating. At half the radius the temperature profile is determined by the neo-classical transport, which scales with $T^{7/2}$ in the long mean free path (LMFP) regime [1]. This unfavourable temperature dependence prohibits high temperatures in non-optimised stellarators for an acceptable heating power. A radial electric field however reduces the neo-classical transport and high temperatures become available. With the localised central power deposition of ECRH a positive radial electric field can be established in the central region [2] and steep temperature gradients with record stellarators electron temperatures of 6.7 keV are achieved. Here the diffusion scales with $\chi_e \propto \sqrt{n_e} T_e^{\frac{5}{4}} E^{-3/2}$ [1]. Usually the transport coefficients are derived from power balance analysis (PBA) and perturbative methods (PM). Assuming a mainly diffusive transport, this means that the diffusion coefficients are determined by the ratio of heat flux over gradient of energy density $\Gamma_{heat} / \nabla(n_e T_e)$ in the case of PBA and $\partial\Gamma_{heat} / \partial(\nabla(n_e T_e))$in the case of PM. This is illustrated in Fig.2, which is representing "Fick´s law". Absolute values of the transport coefficient are known with large error bars only. More reliable are their characteristic dependencies on plasma parameters. In the following experimental investigation we concentrate on the characteristic temperature dependencies to discriminate the different transport regimes.

Experiments

By a proper choice of the resonant magnetic field the ECRH power is deposited locally in the plasma centre within r_{eff}<2 cm. Assuming a mainly diffusive heat transport, the heat flux in Fig. 2 is proportional to the ECRH power for all radii outside the central power deposition zone. The ECRH power was slowly (in 300ms) ramped up and down between **0.2 MW** and **2.1 MW** during the discharge. By this method the heat transport coefficient in Fig.2 can be determined for a variation of the heat flux of an order of magnitude. The temperature and

temperature gradients at different radii are calculated from the electron cyclotron emission spectrum with a magnetic reconstruction of finite β equilibria inclusive Shafranov shift. The other transport relevant plasma parameter were kept constant during the power scan. The density was set to **2.4 10^{19} m^{-3}**. The density profile was flat up to a radius of 13 cm, thus density gradients can be neglected in the transport analysis. In the LMFP-regime the ion temperature profile is energetically decoupled from the electron temperature profile and is rather flat with a maximum of 400 eV. Thus Ion temperature gradients can be neglected, too. The Z_{eff} variation determined from the Bremsstrahlung intensity was estimated to be less than 20 %. Thus only the electron temperature and temperature gradient was changed by the power scan, which make the interpretation simple and reliable. In Fig.2, which is representing Fick´s law, the curves are not straight lines since the diffusion scales with the temperature. To test the right scaling the abscissa is normalised with the different temperature scalings. the best fit was found by a regression analysis. In that case the curve should become a straight line.

First the heat transport at the outer region was investigated. Here the $T^{3/2}$-dependance could be found at radii larger than 11 cm (r/a> 0.6), while for the intermediate region at r_{eff}= 8 cm (r/a= 0.44) the neo-classical $T^{7/2}$-scaling could be derived as shown in Fig.3. The small hysteresis in the signal may originate from the variation of Z_{eff} during the power ramp up and down. Assuming neo-classical transport, the high temperatures and temperature gradients of 6 keV and 1keV/cm in the central region can only be explained by the existence of a radial electric fields. Both the density gradient and the Ion temperature gradient can be neglected in the central region; thus the ambipolar electric field is generated by the electron flux. First we tested weather it can be generated by neo-classical fluxes only. The electric field is then proportional to the temperature gradient. D_{11} and D_{12} are the elements of the neo-classical

$$\Gamma_e = 0 = -n_e\left(D_{11}^e \frac{eE_r}{T_e} + D_{12}^e \frac{\nabla T_e}{T_e} \right) \quad => \quad eE_r = \frac{D_{12}^e}{D_{11}^e} \nabla T_e$$

transport matrix. Their ratio is about 5/4. Thus the heat diffusion coefficient is now also a function of the temperature gradient. With this ansatz no agreement with the experimental data could be found as shown in Fig.4. There is experimental and theoretical evidence that an ECRH-driven suprathermal electron flux plays an important role at least in the formation of electron root feature [2,3]. Therefore in addition to the neo-classical electron flux an ECRH-driven flux was taken into account.

$$\Gamma_{ECRH} \approx \frac{P_{ecrh}^{\alpha}}{E_r^{\frac{3}{2}}} \qquad 0 = \Gamma_{nc} + \Gamma_{ECRH} \Rightarrow E_r(\nabla T_e, T_e, P_{ecrh})$$

From the ambipolarity condition the electric field is also a function of P_{ECRH} and $T^{-1/4}$.

Best agreement (see Fig.4) with the experimental data was found for α =0, which means that the ECRH-driven flux remained constant. The electric field $\mathbf{E_r}$ derived by the regression analyses saturates at a certain value of about 400 V/cm even though the power flux, temperature and temperature gradient are changing by nearly an order of magnitude (see Fig. 5). From an other point of few, the result is, that ratio of

$$\left(\frac{E_r}{r} \right)^{\frac{3}{2}} \approx \frac{\sqrt{n_e} T_e^{\frac{5}{4}}}{\Gamma_{heat}} n_e \nabla T_e = const$$

remains constant for the full power scan.

The radial variation of χ_e was determined by heat wave analysis with a fine resolution Zoom ECE-system. Here additional off- axis ECRH power was deposited at r=8.5 cm with a modulation frequency of 1037 Hz. The sharp radial transition into the electron root region was clearly identified as shown in Fig.5, where χ_e drops by an order of magnitude within a radial layer of about 1 cm width.

Discussion and Conclusion

In the LMFP- regime the electron heat transport at W7-AS is determined by neo-classical transport over a wide range of plasma parameters. In the central region a strong confinement improvement by a positive radial electric field is established with central ECRH above 250 KW. Therefore no fast transition into the electron root regime could be found during the power scan. On the other hand at low temperature the e-root regime hardly differs from the neo-classical transport without E-field. Once the radial electric field is established, it tends to saturate, and no further confinement improvement is achieved. Since it is very unlikely that the ECRH-driven and the grad T driven fluxes balance each other such that E_r remains constant for the whole power scan. This indicates some mechanism, which strongly limits the electrical field strength or the poloidal plasma rotation.

References:

[1] B.B. Kadomtsev, O.P. Pogutse: Nucl. Fusion 11, 67 (1971)

[2] H.Maassberg, et al. : J.Plasma Fusion Res. SERIES, Vol.1 (1998) 122.

[3] S Murakami, et al.: *Proc. 17Th IAEA Fusion Energy Conf., Yokohama1998.* IAEA Vienna 1999, Vol. 4, p.1383

Figures:

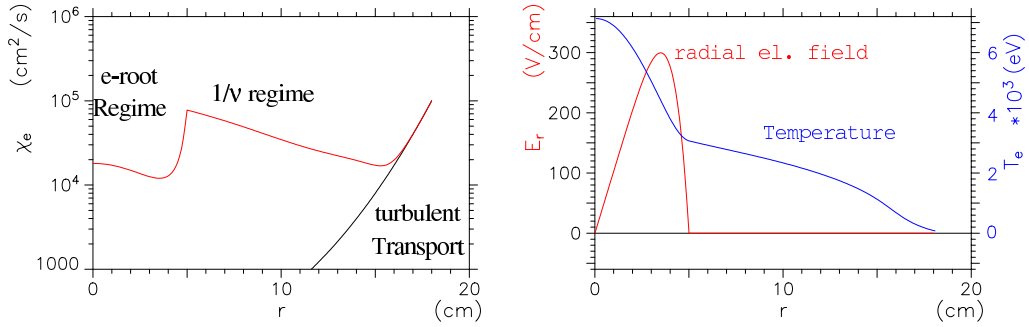

Fig.1 stationary transport simulation (power balance). Left: heat diffusion coefficient. Right: electron temperature profile and electric field profile.

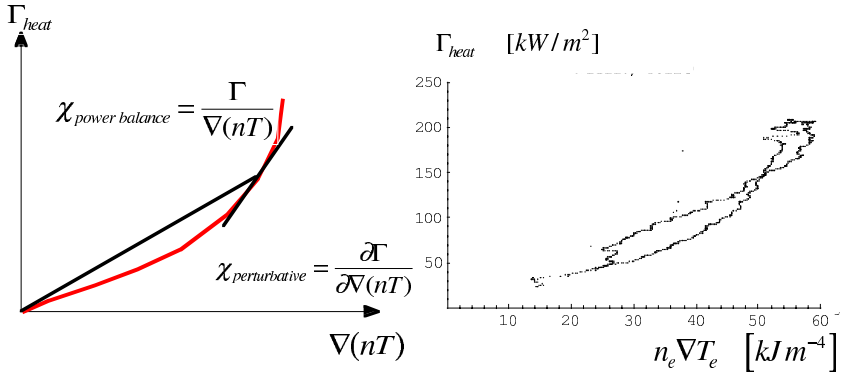

Fig. 2: Left: Schematic representation of the difference between power balance analyses.
Right: Fick´s representation of the measured heat transport at 12 cm (r/a= 0.66).

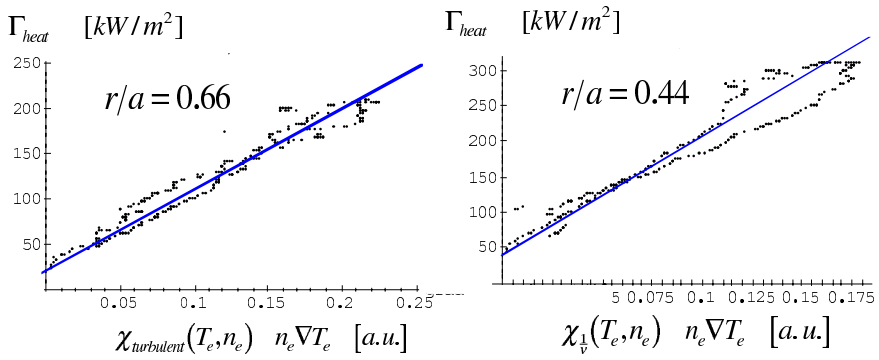

Fig.3: Test of different transport regimes. Left: Turbulent transport with $\chi_e \propto T_e^{\frac{3}{2}}$ *at r/a= 0.66.*
Right: Neo-classical transport with $\chi_e \propto T_e^{\frac{7}{2}}$ *at r/a= 0.44.*

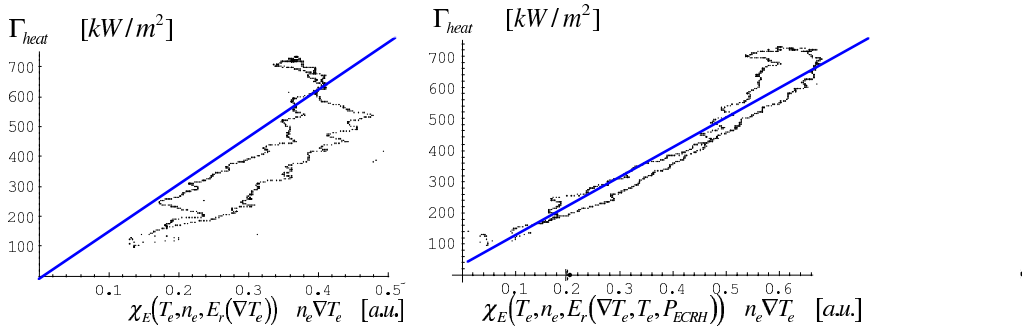

Fig. 4 Left: Assuming that E_ris driven by pure neo-classical fluxes.
Right: Assuming that E_ris generated by an additional ECRH-driven flux .

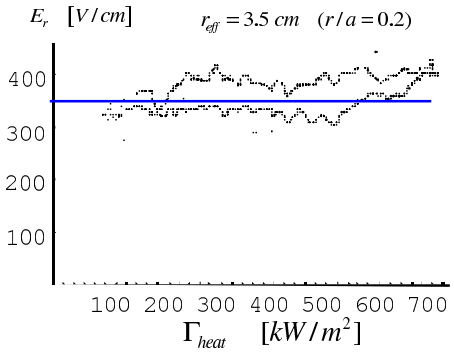

Fig. 5 left: "neo-classical" radial electric field in the e-root region as a function of the heat flux.
right: Phase of heat waves propagating from the outside into the e-root region. The heat diffusion coefficient shows a sharp drop at the radial transition into the e-root region.